Journal of Magnetism and Magnetic Materials 80 (1989) 321–328
North-Holland, Amsterdam

EFFECTS OF CRYSTALLOGRAPHIC ORDERING ON THE MAGNETIC BEHAVIOUR OF $(AgIn)_{1-z}Mn_{2z}Te_2$ AND $(CuIn)_{1-z}Mn_{2z}Te_2$ ALLOYS

G. LAMARCHE, J.C. WOOLLEY

Ottawa-Carleton Institute for Physics, University of Ottawa, Ottawa, Ontario, Canada K1N 6N5

R. TOVAR, M. QUINTERO and V. SAGREDO

Centro de Estudios en Semiconductores, Departamento de Fisica, Universidad de Los Andes, Mérida, Venezuela

Received 20 February 1989

Measurements of magnetic susceptibility in the temperature range 4.2–300 K were made on polycrystalline samples of the $(AgIn)_{1-z}Mn_{2z}Te_2$ and $(CuIn)_{1-z}Mn_{2z}Te_2$ alloys, and the data used to give values of spin-glass transition temperature T_g and Curie–Weiss paramagnetic temperature Θ. For any sample for which the X-ray powder photograph indicated an apparently single phase condition, either zinc-blende or chalcopyrite, the susceptibility data could show up to three separate T_g values. These different magnetic conditions are attributed to crystallographic ordering of the Mn ions on the chalcopyrite and zinc-blende lattices, the three observed T_g values corresponding to disordered zinc-blende, ordered zinc-blende and ordered chalcopyrite. The value of Θ obtained from the $1/\chi$ vs. T plot is shown to be a weighted mean of the separate values of Θ for the phases present. The relative sizes of the T_g peaks and the values of Θ for any given sample gives an indication of the amount of each phase present. These amounts were varied by using different methods of heat treatment and it was shown that the magnetic behaviour was consistent with the $T(z)$ phase diagram for the two alloy systems.

1. Introduction

Most of the work [1,2] on semimagnetic semiconductor alloys has been concerned with alloys of the form $II_{1-z}Mn_zVI$. However similar alloys can be produced from the chalcopyrite $I.III.VI_2$ compounds, the ternary analogs of the II.VI compounds. The crystallography and optical energy gap values of a number of alloy systems of the form $(I.III)_{1-z}Mn_{2z}Te_2$ have been investigated [3–6] and the work has also been extended to the more general $Cd_{2x}(I.III)_yMn_{2z}Te_2$ $(x+y+z=1)$ alloys [7,8]. Preliminary magnetic results on a range of $(I.III)_{1-z}Mn_{2z}Te_2$ alloys have been reported [9].

These chalcopyrite-based alloys are of interest because, depending upon the heat-treatment, the alloys can be produced either with the Mn atoms distributed at random on the chalcopyrite or zinc-blende cation sublattices or with extra ordering effects occurring in these lattices. It is found that the optical energy gap values and the magnetic behaviour are very different for the two different conditions [3,7,8]. Thus, the parameters obtained from measurements of magnetic susceptibility will depend upon the particular heat-treatment of the samples measured. In the present work, samples of $(AgIn)_{1-z}Mn_{2z}Te_2$ and $(CuIn)_{1-z}Mn_{2z}Te_2$ with various values of z have been produced under various conditions of heat-treatment and the resulting magnetic behaviour investigated.

2. Preparation of samples and experimental measurements

The alloys used were produced by the usual melt and anneal technique [10]. The components of each 1 g sample were sealed under vacuum in small quartz ampoules which had previously been carbonized to prevent interaction of the alloy with

0304-8853/89/$03.50

the quartz, and were melted together at 1150 °C. These samples were then annealed for 20 to 30 days at 600 °C to give homogeneity, the data obtained previously for the $T(z)$ phase diagrams [3] showing that this temperature was satisfactory for this purpose. The samples were then variously treated to give a range of materials showing different amounts of order. Details of the particular heat-treatments will be given below. In every case, at the end of the heat-treatment, X-ray powder photographs, either Debye–Scherrer or Guinier, were taken to indicate the condition of the sample before magnetic measurements were made.

For the lower range of temperature, magnetic susceptibility measurements were made (in Ottawa) with a SQUID magnetometer for magnetic fields in the range 1 to 2.5 mT and over a temperature range from 4.2 to 200 K. For the measurements of the Curie–Weiss 'paramagnetic' temperature in the range from 80 to 300 K, measurements of magnetic susceptibility were made (in Mérida) using a Faraday magnetometer with a constant field gradient of 3.43 T/m and an external magnetic field of up to 0.6 T.

3. Results

As is well known, for these semimagnetic semiconductor materials, the values of magnetic susceptibility χ plotted as function of temperature T should show a well defined cusp at the critical temperature T_g. Practically all of the samples investigated here showed this type of behaviour, but for the majority of the samples, more than one such cusp was observed. This indicated the presence of more than one magnetic phase in such a sample. However, since the X-ray photograph in each case showed only a single phase, either zinc-blende or chalcopyrite, as has been discussed previously [7,8], the presence of different magnetic phases has been attributed to ordering of the different cations on the cation sublattice of the basic zinc-blende or chalcopyrite structure. Study of the $T(z)$ phase diagrams of the $(AgIn)_{1-z}Mn_{2z}Te_2$ and $(CuIn)_{1-z}Mn_{2z}Te_2$ systems [3] indicates that the relevant ordering temperatures are relatively low and so any given sample is likely to show some ordered and some disordered regions, the relative amounts of each depending upon the exact annealing and cooling conditions used. This is illustrated in fig. 1, where the curves of χ vs. T are shown for two samples of composition AgIn $z = 0.5$, one of which was quenched from 600 °C and the other very slowly cooled to room temperature. It is to be noted that the X-ray photographs for these two samples appeared identical, both indicating a single phase zinc-blende structure, with equal lattice parameters. It is seen that the strong peak at 20 K in the quenched sample has almost disappeared in the slowly cooled sample, but that this latter shows a strong peak at 29 K and a smaller peak at 47 K. In view of the $T(z)$ diagram [3], the peak at 20 K is attributed to the disordered zinc-blende β phase while the peak at 29 K is attributed to the ordered zinc-blende β' phase. As will be discussed below, the peak at 47 K corresponds to the ordered chalcopyrite α' phase.

In order to determine the values of the various critical temperatures T_g, samples were annealed at various temperatures in the range 200–600 °C and quenched to room temperature and also cooled at

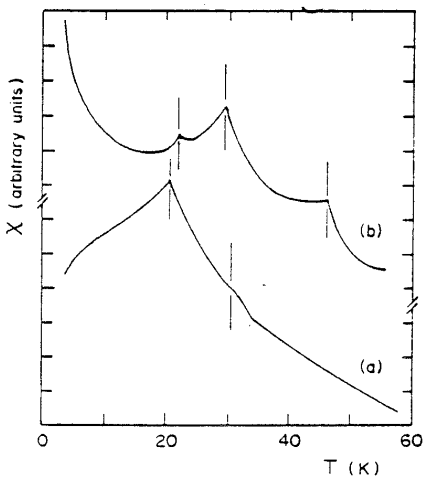

Fig. 1. Variation of magnetic susceptibility χ with temperature T for the alloy $(AgIn)_{1-z}Mn_{2z}Te_2$ with $z = 0.5$. (a) Water-quenched from 600 °C; (b) very slowly cooled to room temperature.

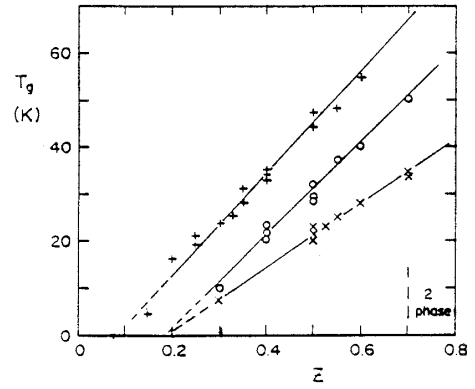

Fig. 2. Variation of spin-glass temperature T_g with composition z for $(AgIn)_{1-z}Mn_{2z}Te_2$ alloys. × disordered zinc-blende (T_{g1}); ○ ordered zinc-blende (T_{g2}); + ordered chalcopyrite (T_{g3}).

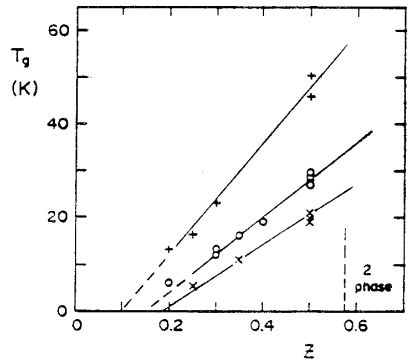

Fig. 3. Variation of spin-glass temperature T_g with composition z for $(CuIn)_{1-z}Mn_{2z}Te_2$ alloys. × disordered zinc-blende (T_{g1}); ○ ordered zinc-blende (T_{g2}); + ordered chalcopyrite (T_{g3}).

various rates from 600° to room temperature. The resulting values of critical temperature T_g for the AgIn alloys are shown in fig. 2. It is seen that the points clearly divide into three sets corresponding to i) the disordered zinc-blende β structure (T_{g1}), ii) the ordered zinc-blende β' structure (T_{g2}) and iii) the ordered chalcopyrite α' structure (T_{g3}). It is seen that no zinc-blende data were obtained for $z < 0.3$, partly due to the low values of T_{g1} in this range, but mainly because the samples with $z < 0.3$ were largely chalcopyrite, as seen from the X-ray data. Also it was found that reasonable sized peaks corresponding to the disordered zinc-blende phase were obtained only for samples water-quenched from temperatures of 500–600 °C. (see fig. 1). Even with air-quenching, ordering took place during the cooling process, and the main peak observed corresponded to the ordered zinc-blende T_{g2}. Values for T_{g3} were obtained in the range $0.15 < z < 0.35$, confirming that T_{g3} was characteristic of the chalcopyrite structure. No peaks were observed for any alloy corresponding to a disordered chalcopyrite structure.

The corresponding results for the CuIn alloys are shown in fig. 3. Fewer data were obtained in this case, but the points again clearly divide into the same three sets of disordered zinc-blende, ordered zinc-blende and ordered chalcopyrite. In these alloys, even the water-quenched samples showed a strong peak corresponding to the ordered zinc-blende T_{g2}, and the disordered T_{g1} peak was small, if observed at all, indicating that it was very difficult to retain the disordered zinc-blende phase down to room temperature, even with water-

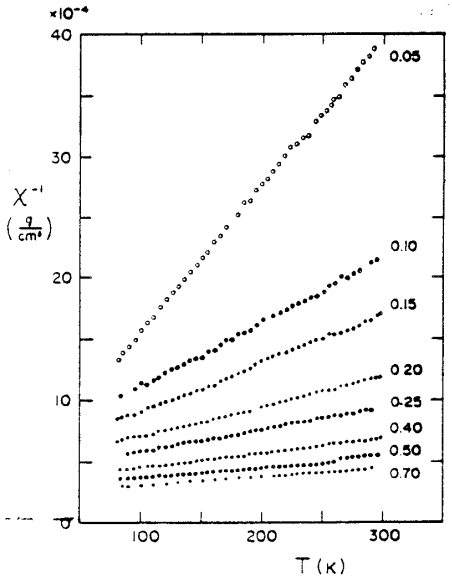

Fig. 4. Variation of reciprocal magnetic susceptibility χ^{-1} with temperature T for water-quenched $(AgIn)_{1-z}Mn_{2z}Te_2$ alloys – values of z shown for each line.

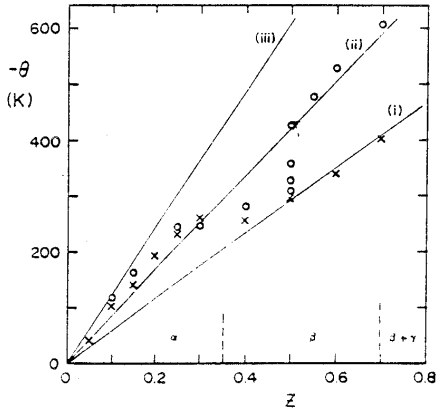

Fig. 5. Variation of Curie–Weiss temperature Θ with composition z for $(AgIn)_{1-z}Mn_{2z}Te_2$ alloys. × experimental values – water-quenched samples; ○ experimental values – more slowly cooled samples; ——— predicted values, (i) disordered zinc-blende, (ii) ordered zinc-blende, (iii) ordered chalcopyrite. Phase fields shown represent equilibrium condition at 400 °C, α chalcopyrite, β zinc-blende.

quenching. Again no examples of a disordered chalcopyrite phase were obtained.

The other magnetic parameter of interest which can be determined from the magnetic susceptibility measurements is the Curie–Weiss paramagnetic temperature Θ. For temperatures well above T_g, the samples should show the normal Curie–Weiss behaviour of $\chi = C/(T - \Theta)$, so that graphs of $1/\chi$ vs. T should be straight lines giving Θ as the T intercept. For a set of AgIn samples having various z values and water-quenched from 600 °C, the variation of $1/\chi$ vs. T in the range 80 K < T < 300 K is shown in fig. 4. Straight lines drawn through these points gave the values of Θ which are shown in fig. 5. Values of Θ for other heat treatments are also shown in fig. 5. In particular, for the case of $z = 0.5$, Θ was determined for samples which were cooled at various rates. It was found that the slower the cooling rate, the higher the observed value for $-\Theta$, and while the water-quenched sample had $\Theta = -295$ K, the very slowly cooled sample giving the data shown in fig. 1 had a Θ value of -420 K. Corresponding results for the CuIn alloys are shown in fig. 6 and again for $z = 0.5$ the observed $-\Theta$ was found to

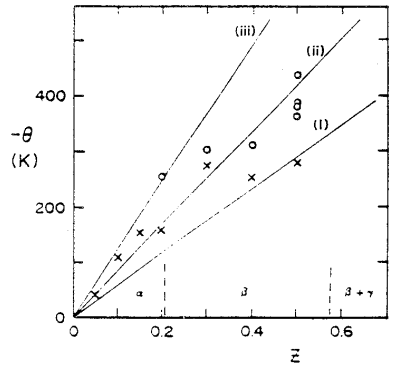

Fig. 6. Variation of Curie–Weiss temperature Θ with composition z for $(CuIn)_{1-z}Mn_{2z}Te_2$) alloys. × experimental values – water-quenched samples; ● experimental values – more slowly cooled samples; ——— predicted values, (i) disordered zinc-blende, (ii) ordered zinc-blende, (iii) ordered chalcopyrite. Phase fields shown represent equilibrium condition at 400 °C, α chalcopyrite, β zinc-blende.

increase as the rate of cooling from 600 °C used in the production of the alloys was decreased.

It is clear that in the case of Θ, no separate sets of points are obtained as with T_g. This is to be expected since while an alloy with mixed phases will give the separate values of T_g for each phase, the Θ values obtained will be some average of the

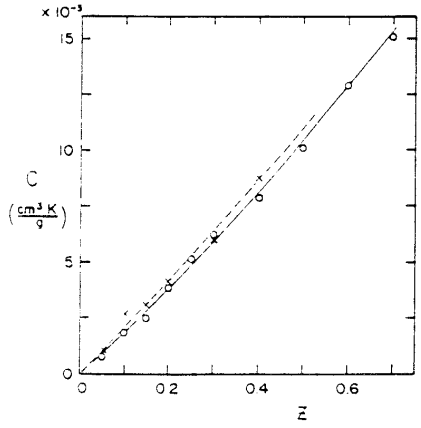

Fig. 7. Variation of Curie constant C with composition z. $(AgIn)_{1-z}Mn_{2z}Te_2$ values, ● measured, ——— predicted; $(CuIn)_{1-z}Mn_{2z}Te_2$ values, × measured, - - - - - - predicted.

values corresponding to the separate phases. This will be discussed further below.

The other parameter obtained from the graphs in fig. 4 is C and values of C for both the AgIn and CuIn alloys are shown as a function of z in fig. 7, where C is in units of cm^3K/g. For Curie–Weiss behaviour, theory gives C in this form as

$$C = zN_A g^2 \mu_B^2 S(S+1)/3kW, \qquad (1)$$

where N_A is Avogadro's no. and W the molecular weight. Assuming $g = 2$ and $S = 5/2$, lines can be calculated for the two alloy system concerned and these are shown in fig. 7. It is seen that within the limits of experimental error, the measured values of C agree with these calculated values.

4. Discussion and analysis

As indicated above, the T_g values in figs. 2 and 3 divide into three sets, corresponding to disordered zinc-blende (T_{g1}), ordered zinc-blende(T_{2g}) and ordered chalcopyrite (T_{3g}). From a consideration of the $T(z)$ phase diagram (fig. 9) and the variation of χ vs. T curve with heat treatment, the allocation of T_{g1} and T_{g2} is reasonably clear. However, since only one chalcopyrite phase is observed in the magnetic data, the allocation of T_{g3} to the ordered condition needs to be explained. The $T(z)$ diagram indicates that this is likely, but the deciding factor is the variation of optical energy gap E_0 with z. As shown previously, the lines of E_0 vs. z extrapolate at $z = 1$ to values of E_0 which are characteristic of the particular structures. In the case of AgIn alloys [3,8], the line of E_0 vs. z in the composition range $0 < z < 0.1$ has an aiming point at $z = 1.0$ in the energy range 2.3–2.8 eV, but in the composition range $0.1 < z < 0.35$, the aiming point is 1.35 eV. These results combined with the $T(z)$ data indicate that for $0 < z < 0.1$ the alloys are mainly disordered, but for $0.1 < z < 0.35$ the dominant phase is the ordered chalcopyrite structure.

One further point concerning T_{g3} is that values of this parameter are observed at z values up to 0.6 for very slowly cooled samples. This indicates that the ordered chalcopyrite structure occurs at these higher z values, a result not shown by the initial $T(z)$ diagram [3]. This is discussed further below.

The behaviour of the disordered zinc-blende phase should be very similar to that of the $Cd_xZn_yMn_zTe$ alloys previously investigated [11]. In that case, it was shown that the exchange interaction was dominated by superexchange due to virtual transitions between the valence band and a delocalized band of $3d^5$ states. This mechanism gives the exchange parameter between two Mn ions spaced a distance r as [12]

$$J(r) = I_0 r^{-2} \exp(-\alpha r) \qquad (2)$$

with α proportional to $\epsilon^{1/2}$ where ϵ is the energy difference in the virtual transition. For a random distribution of Mn ions on the cation sublattice, it is shown [12] that

$$\ln\left(d^2 T_g z^{-2/3}\right) = \ln(-AI_0/k) - \alpha d z^{-1/3}, \qquad (3)$$

where d is the nearest neighbour cation spacing and $A = S(S+1)$, with $S = 5/2$ for the Mn ions and $d = a/\sqrt{2}$ for zinc-blende, where a is the lattice parameter.

The values of T_{g1} for the AgIn alloys can be analyzed in this way, the values of lattice parameter having been given previously [3,8]. Fig. 8 shows the variation of $\ln(d^2 T_{g1} z^{-2/3})$ with $az^{-1/3}$ for these alloys. The difficulty discussed above of obtaining good samples of the disordered alloys results in a limited number of T_{g1} values being

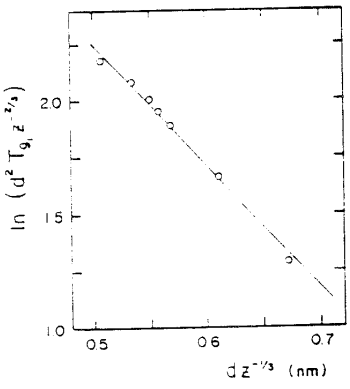

Fig. 8. Variation of $\ln(d^2 T_{g1} z^{-2/3})$ with $dz^{-1/3}$ for $(AgIn)_{1-z}Mn_{2z}Te_2$ alloys.

obtained. Also, as was shown for the $Cd_xHg_yMn_zTe$ alloys [13], for values of energy gap E_0 smaller than 1.5 eV, there is some contribution to J from the Bloembergen–Rowland exchange mechanism, this contribution being larger the smaller the value of E_0. For the present alloys, the contribution should not exceed approximately 15% of J but it will vary with z because of the variation of E_0. Thus, the parameters obtained from the data in fig. 8 will represent some mean value over the composition range used. From fig. 8, the values obtained are $\alpha = (5.4 \pm 0.1)$ nm^{-1} and $AI_0/k = -(1.38 \pm 0.2) \times 10^2$ Knm^2. These values are somewhat different from those for zinc-blende obtained from various $II_{1-z}Mn_zTe$ alloys [11,14], but the difference may be due to the inclusion of a Bloembergen–Rowland contribution, as indicated above.

One other parameter which can be obtained from the graphs in figs. 2 and 3 is the nearest neighbour percolation limit, given by the extrapolation of the linear region of the T_g vs. z graphs to $T_g = 0$. For the disordered zinc-blende T_{g1} data, the lines are consistent with a limit of $z = 0.19$, the theoretically predicted value [15]. For T_{g2}, the ordered zinc-blende structure, the AgIn alloys give a value close to 0.19, but for the CuIn case, for which fewer data are available, the value appears closer to 0.15. Finally, for the ordered chalcopyrite T_{g3}, both AgIn and CuIn alloys give a value close to 0.10. Since the ordered structures have not as yet been definitely determined, a theoretical value for the percolation limit in these cases cannot be found. However, it appears probable [3,6] that the ordered structures are based on a stannite-like ordering, with the Mn ions occupying sites in alternate planes of cations. This would essentially increase the concentration of Mn ions in these planes compared with the disordered case, and hence the percolation limit could be expected to be lower.

Once the values of α and AI_0/k have been determined for the disordered zinc-blende structure as indicated above, it is possible to calculate the variation of Θ with z for that structure. Standard mean field theory [16] gives

$$\Theta = (2S(S+1)/3k) \sum_i n_i J_i, \qquad (4)$$

where Σ_i represents the summation over consecutive sets of neighbours, i.e. $i = 1$ for nearest neighbours, 2 for next nearest neighbours etc., n_i is the number of neighbours in each set and J_i the appropriate value of the exchange parameter. With J_i given by eq. (2) and a concentration of paramagnetic ions z, so that n_i is replaced by zn_i, then

$$\Theta = (2S(S+1)I_0 z/3k) \sum_i n_i \exp(-\alpha r_i)/r_i^2. \qquad (5)$$

For zinc-blende, the values of n_i for successive values of i are 12, 6, 24, 12, 24, 8, 48 [11]. Using the values of α, I_0 and S given above and the measured values of a [3], it is found that the variation of a has negligible effect and that $\Theta = -594z$. This line is shown in fig. 5.

A similar calculation cannot be carried out for either of the ordered structures since the values of α and AI_0/k are not known. However, approximate lines can be drawn for these if it is assumed that for any given composition Θ is proportional to T_{g1} since both are determined by the value of $J(r)$. Thus, in order to give approximate lines, it has been assumed that for $z = 0.5$ $\Theta_2 = T_{g2}\Theta_1/T_{g1}$ and $\Theta_3 = T_{g3}\Theta_1/T_{g1}$, and lines have been drawn from the origin through these points as shown in fig. 5.

A similar analysis to that given above should be used for the CuIn alloys. However, because of the difficulty in retaining the disordered phase at room temperature, as discussed above, insufficient values of T_{g1} were obtained to give a graphical form of eq. (3) of any accuracy. Therefore, the three θ lines drawn for the AgIn alloys in fig. 5 have been repeated for the CuIn alloys in fig. 6.

The measured Θ values will be a weighted average of the values corresponding to the phase present. Thus, consider the case when an alloy consists of a fraction f of phase p and $(1-f)$ of phase q. Then the measured χ value will be

$$\chi = \frac{fC}{T-\Theta_p} + \frac{(1-f)C}{T-\Theta_q}. \qquad (6)$$

Hence

$$\frac{1}{\chi} = \frac{(T-\Theta_p)(T-\Theta_q)}{C(T-\Theta_p+f\delta)}, \qquad (7)$$

where $\delta = \Theta_p - \Theta_q$.

If Θ_S is defined as $\Theta_S = f\Theta_p + (1-f)\Theta_q$, it can be shown that

$$\frac{1}{\chi} = \frac{1}{C}\Big\{(T-\theta_S) + \big\{T(\Theta_S-\Theta_q) - f\delta(T-\Theta_S) - \Theta_p(\Theta_S-\theta_q)\big\}\big\{T-\Theta_p+f\delta\big\}^{-1}\Big\}$$

and hence

$$\frac{1}{\chi} = \frac{1}{C}\left\{(T-\Theta_s) - \frac{f(1-f)\delta^2}{(T-\theta_S)-\delta(1-2f)}\right\}.$$

Writing $1/\chi = (T-\Theta_m)/C$ where Θ_m is the measured value

$$\Theta_m = \Theta_S + \frac{f(1-f)\delta^2}{(T-\Theta_S)-\delta(1-2f)} = \Theta_S + A(T). \tag{8}$$

It is seen that because of the term $A(T)$, the variation of $1/\chi$ vs. T will not be linear. However, in the present case, if p is taken as the disordered zinc-blende phase and q the ordered zinc-blende phase, the predicted values of Θ in fig. 5 indicate that in the temperature range concerned here $A(T)$ will never exceed 5% of Θ_S. Thus, to a good approximation, the line of $1/\chi$ vs. T can be treated as straight and the resulting measured Θ_m is given by

$$\Theta_m = f\Theta_1 + (1-f)\Theta_2, \tag{9}$$

where f and $(1-f)$ are the fractions of disordered zinc-blende and ordered zinc-blende in the sample. The analysis is more complicated if all three phases – disordered zinc-blende, ordered zinc-blende and ordered chalcopyrite – are present, but again to a good approximation in this case $\Theta_m = f_1\Theta_1 + f_2\Theta_2 + f_3\Theta_3$ with $(f_1+f_2+f_3) = 1$.

The values of Θ shown in figs. 5 and 6 are explained by these relations. Clearly, all measured values should lie between the ordered chalcopyrite and disordered zinc-blende lines. This conditions is satisfied in the AgIn case by all but the water-quenched samples with $z = 0.6$ and 0.7. These points lie just below the disordered zinc-blende line, but bearing in mind the approximations made in determining this line, the results are satisfactory. A similar conclusion can be made about the CuIn results in fig. 6. The measured values of Θ give a good indication of the relative concentrations of the different structures in any given sample, and this can then be correlated with the heat treatment used to produce the sample. Discussion of this correlation requires the $T(z)$ phase diagram considered below.

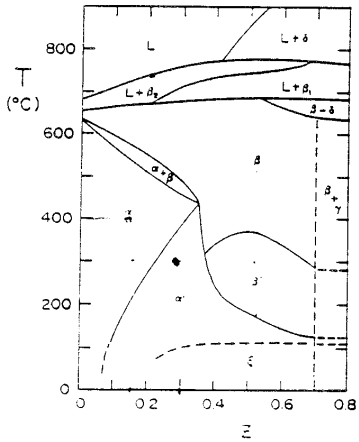

Fig. 9. $T(z)$ phase diagram for $(AgIn)_{1-z}Mn_{2z}Te_2$ alloys. α disordered chalcopyrite; α' ordered chalcopyrite; β disordered zinc-blende; β' ordered zinc-blende; γ MnTe with NiAs structure; ξ phase condition not yet determined.

As indicated above, in the AgIn and CuIn $T(z)$ phase diagrams presented previously [3], it was assumed in both cases that the limit of the chalcopyrite α field was less than $z = 0.4$. However, the present magnetic measurements on very slowly cooled samples indicate that the chalcopyrite phase can be obtained in both diagrams at $z = 0.5$ and 0.6. Thus, the DTA measurements in this composition range were repeated with careful study given to the data in the range 100–300 °C. This work will be described elsewhere [17], but the AgIn $T(z)$ diagram is given here in fig. 9 so that the variation of the measured Θ values can be discussed.

Considering the AgIn alloys, it would be expected that in the composition range $0 < z < 0.3$, the samples would have chalcopyrite structure and that little, if any, zinc-blende phase would be present. Thus, particularly in the range $0 < z < 0.2$,

the difference in Θ between water-quenched and slowly cooled samples would have to be attributed to varying amounts of disordered chalcopyrite phase. However, in this range the values of Θ are small, and so any difference would be small. Also, because of the lower temperature limit of 4.2 K to the T_g measurements, disordered chalcopyrite samples with $z < 0.2$ would probably have too low a T_g value to be observed. In the range $0.2 < z < 0.3$, from the $T(z)$ diagram the samples would be expected to be ordered chalcopyrite regardless of heat-treatment, and the Θ values from water-quenched and slow cooled samples are in the fact very similar in this range. The values are not as large as on the predicted ordered chalcopyrite line, and this would seem to indicate that the values for this line have been over-estimated. At $z = 0.35$, there is a very rapid fall in the temperature of the zinc-blende β to chalcopyrite α' transition, and so for $z > 0.35$, samples would be expected to be mainly of zinc-blende structure. For the water-quenched samples, this is clearly true and the Θ values lie very close to the predicted disordered zinc-blende values. The effect of slower cooling rates is illustrated by the various Θ values at $z = 0.5$. As indicated above, it was found that the slower the cooling rate the larger the value of $-\Theta$ observed i.e. the larger the fraction of ordered phase present. From the $T(z)$ diagram, it is clear that the time spent within 100 °C or so below the ordering ($\beta \rightarrow \beta'$) temperature will be the main factor in determining the fraction of ordered phase. Finally, a set of very slowly cooled samples were produced in the range $0.5 < z < 0.7$, the latter value being the limit of single phase behaviour. In these cases, the T_g data indicate that some chalcopyrite ordered phase is present, and the measured Θ values are in agreement with this. The amount of chalcopyrite phase present is likely to be small, since the $\beta' \rightarrow \alpha'$ boundary lies between 200 and 130 °C, so that slow rates of phase conversion are to be expected. This is reflected in the values of Θ measured. The DTA data indicate the possible occurrence of one even lower phase boundary at approximately 100–130 °C. It is planned to use magnetic measurements to obtain information on this possible phase change in further work.

The discussion given above for the AgIn alloys applied equally well to the data for the CuIn alloys shown in fig. 6.

Acknowledgements

The Canadian authors wish to thank Laura Dierker and Riccardo Brun del Re for assistance with the magnetic measurement. The Venezuelan authors are grateful to Consejo de Desarrollo Científico y Tecnologico (CDCHT) and Consejo Nacional de Investigaciones Científicas y Tecnologicas (CONICIT) for financial support.

References

[1] J.A. Gaj, J. Phys. Soc. Japan 49 (1980) 797.
[2] J.K. Furdyna, J. Appl. Phys. 53 (1982) 7637.
[3] M. Quintero, P. Grima, R. Tovar, G.S. Pérez and J.C. Woolley, Phys. Stat. Sol. (a) 107 (1988) 136.
[4] M. Quintero, R. Tovar, M. Al-Najjar, G. Lamarche and J.C. Woolley, J. Solid State Chem. 75 (1988) 136.
[5] M. Quintero, P. Grima, R. Tovar, R. Goudreault, D. Bissonnette, G. Lamarche and J.C. Woolley, J. Solid State Chem. (in press).
[6] A. Aresti, L. Garbato, A. Geddo-Lehmann and P. Manca, Proc. 7th Intern. Conf. on Ternary and Multinary Compounds (Materials Research Society, 1986) p. 497.
[7] M. Quintero, L. Dierker and J.C. Woolley, J. Solid State Chem. 63 (1986) 110.
[8] M. Quintero and J.C. Woolley, Phys. Stat. Sol. (a) 92 (1985) 449.
[9] J.C. Woolley, G. Lamarche, A. Manoogian, M. Quintero, L. Dierker, M. Al-Najjar, D. Proulx, C. Neal and R. Goudreault, Proc. 7th Intern. Conf. on Ternary and Multinary Compounds (Materials Research Society, 1986) p. 479.
[10] R. Brun del Re, T. Donofrio, J.E. Avon, J. Majid and J.C. Woolley, Nuovo Cimento D2 (1983) 1911.
[11] J.C. Woolley, S.F. Chehab, T. Donofrio, S. Manhas, G. Lamarche and A. Manoogian, J. Magn. Magn. Mat. 61 (1986) 13.
[12] W. Geertsma, C. Haas, G.A. Sawatzky and G. Vertogen, Physica B 86–88 (1977) 1039.
[13] D.J.S. Beckett, S.F. Chehab, G. Lamarche and J.C. Woolley, J. Magn. Magn. Mat. 69 (1987) 311.
[14] S. Manhas, K.C. Khulbe, D.J.S. Beckett, G. Lamarche and J.C. Woolley, Phys. Stat. Sol. (b) 148 (1987) 267.
[15] G.S. Grest and E.G. Gabl, Phys. Rev. Lett. 43 (1979) 1183.
[16] J.S. Smart, Magnetism, vol. III, eds. G.T. Rado and H. Suhl (Academic Press, New York, 1963) p. 63.
[17] M. Quintero, F. Sanchez, M. Dhesi and J.C. Woolley, submitted.